ARL-TR-8409 ● JULY 2018

US Army Research Laboratory

Meander-Line Resonator Designs for 20- to 90-MHz Soil Permittivity Measurements

by Christopher S Kenyon

NOTICES

Disclaimers

The findings in this report are not to be construed as an official Department of the Army position unless so designated by other authorized documents.

Citation of manufacturer's or trade names does not constitute an official endorsement or approval of the use thereof.

Destroy this report when it is no longer needed. Do not return it to the originator.

ARL-TR-8409 ● JULY 2018

US Army Research Laboratory

Meander-Line Resonator Designs for 20- to 90-MHz Soil Permittivity Measurements

by Christopher S Kenyon
Sensors and Electronic Devices Directorate, ARL

REPORT DOCUMENTATION PAGE

Form Approved
OMB No. 0704-0188

1. REPORT DATE *(DD-MM-YYYY)*	2. REPORT TYPE	3. DATES COVERED (From - To)
July 2018	Technical Report	1 October 2017–8 June 2018

4. TITLE AND SUBTITLE
Meander-Line Resonator Designs for 20- to 90-MHz Soil Permittivity Measurements

5a. CONTRACT NUMBER

5b. GRANT NUMBER

5c. PROGRAM ELEMENT NUMBER

6. AUTHOR(S)
Christopher S Kenyon

5d. PROJECT NUMBER

5e. TASK NUMBER

5f. WORK UNIT NUMBER

7. PERFORMING ORGANIZATION NAME(S) AND ADDRESS(ES)
US Army Research Laboratory
ATTN: RDRL-SER-U
Aberdeen Proving Ground, MD 21005-5066

8. PERFORMING ORGANIZATION REPORT NUMBER
ARL-TR-8409

9. SPONSORING/MONITORING AGENCY NAME(S) AND ADDRESS(ES)
Joint Improvised-Threat Defeat Organization
8725 John J. Kingman Road, Stop 6201
Fort Belvoir, VA 22060-6201

10. SPONSOR/MONITOR'S ACRONYM(S)
JIDO

11. SPONSOR/MONITOR'S REPORT NUMBER(S)

12. DISTRIBUTION/AVAILABILITY STATEMENT
Approved for public release; distribution is unlimited.

13. SUPPLEMENTARY NOTES

14. ABSTRACT
We created new computer designs of meander-line resonators for soil permittivity measurement that are able to measure down to the 20-MHz decade and cover the 20- to 90-MHz range. The designs, subject to the condition of 50-Ω line impedance, were derived by successive modifications of a 250-MHz line resonator model guided by computational electromagnetic modeling. Use of a higher dielectric substrate separating the resonator circuits from their grounding plane produced stronger and more-distinct resonances in addition to a far smaller and more practical footprint than with a lower dielectric substrate. In order to lower resonator operational frequency, it became necessary to increase substrate thickness because a lower bound on operational frequency was found that was an increasing linear function of the inverse of substrate thickness. Using measured permittivities of Yuma, Arizona, soils with several water contents from 2.5% to 15% for the modeling, designs performed best with our driest soil. Designs with fewer meander loops produced more-usable resonances for moister soils. Computed parameters for permittivity determination of homogeneous dielectric samples agreed with model-specified permittivity for sample depths of 25 mm or more but were unreliable for sample depths less than about 5 mm due to resonance nonlinearities.

15. SUBJECT TERMS
meander line, ring, resonator, soil, permittivity, measurement, VHF, computational, electromagnetic, modeling

16. SECURITY CLASSIFICATION OF:			17. LIMITATION OF ABSTRACT	18. NUMBER OF PAGES	19a. NAME OF RESPONSIBLE PERSON
a. REPORT	b. ABSTRACT	c. THIS PAGE			Christopher S Kenyon
Unclassified	Unclassified	Unclassified	UU	41	19b. TELEPHONE NUMBER (Include area code) 301-394-5547

Contents

List of Figures

List of Tables

1. Introduction

The US Army is pursuing the use of radar to detect targets in the ground. In an effort to penetrate deeper into the ground, radars in the VHF frequency range are of interest. To determine radar's penetration capability and to better identify and locate targets with a radar system, knowledge of the dielectric properties of soil within its operating frequency band is necessary.

In pursuit of soil permittivity measurements in the 20- to 90-MHz range, we created computer models of new permittivity sensors using the meander-line ring-resonator concept reported in Mazzaro et al.[1] When a ring resonator is loaded with soil its resonance frequencies and quality factors (Q's) reduce. The permittivity is computed from the changes in these two parameters from the soil relative to the unloaded sensor case.

High-frequency ring resonators used a ring for the resonator, but for lower frequencies as Mazzaro used, he meandered the ring to increase its length without increasing its areal footprint. This change transformed the "ring" resonator into a "meander-line" resonator.

Computer modeling using FEKO computational electromagnetic (EM) software[2] allowed for investigations into different designs and the subsequent prediction of whether a low-frequency resonator was possible and practical. We used the Method of Moments (MoM) algorithm in FEKO to compute the resonator response at each frequency. By altering model parameters and extending the geometry of new circuit designs, we found a collection of models that could perform at the lower band frequencies of interest and serve as a guide for building a new resonator. Additional descriptions for building a complete resonator system would follow from those used in the original 250-MHz resonator described in the Mazzaro report[1] but with adjustments for the larger sizes, new permittivity lookup tables, and software for the new frequency range. This report covers the computed results of successively modified resonator models starting from the original 250-MHz meandered-line resonator to modified models whose first resonance, F_o, unloaded by soil, was as low as 24 MHz.

Additionally, we used FEKO simulations to determine how much dielectric sample depth would be sufficient to accurately match the modeled soil permittivity. In practice, this information is needed both to calibrate the measurement system with known dielectrics and for cases where only a limited volume of soil might be available. Although the simulation calculation assumes an infinite depth of soil, the fields and currents responsible for the effect by which the sensor work occur only

within a limited distance from the sensor. We want the sensor to measure just the sample and not the effect of the air above it. Certainly, if one were to measure a layer of soil too thin, air would be in range of the fields thereby altering the permittivity to be measured. The simulations suggest soil depths as low as 25 mm result in measurements 98% or 99% in agreement with modeled permittivities. For the case of the sensor faced down into the earth, these sample depth simulations also give an idea of how deep into the soil the sensors sense the permittivity.

2. Methodology

A top view of the 250-MHz meandered-line ring resonator developed by Mazzaro et al.,[1] is depicted in the FEKO computer model shown in Fig. 1. A side view diagram looking into an input line is shown in Fig. 2. The resonator circuit consists of a closed loop strip line, symmetric about a line passing through the two input/output (I/O) conducting strip line leads that are connected to lines conformal to the resonator loop strip line but slightly separated from it by a gap as can be seen in Fig. 1. These three circuits overlie a dielectric substrate above a conductive ground plane as depicted in Fig. 2. The separation gap between the two I/O, or port, circuit lines from the central resonator loop permits EM coupling from the input strip line, excited by RF input, to the loop. In practice, the RF voltage source depicted in Fig. 2 by the thin cylinder connecting the ground plane to the input strip line would actually be a cable supplying the RF excitation with one side connected to the input line and the other to the ground plane. The loop, having received RF energy that covers our band of interest, then resonates at its resonance frequencies reflecting its effective dielectric environment. The excitement of the loop is then communicated to the output by EM coupling across the second gap to the output line. The output was then passed to a network analyzer that was not modeled in this study. In a physical measurement, the ratio of the voltage at the output port to the voltage at the input port, or network S_{21} parameter, of the sensor versus frequency would appear on the network analyzer. In our computer modeling we plot the S_{21} for the sensor network computed by FEKO. In Fig. 2 the soil is shown on top of the resonator circuit face as it might be for measurement of a limited soil sample or a calibration slab; however, in practice, it is usually operated upside down so that its circuit is face down in contact with the soil.

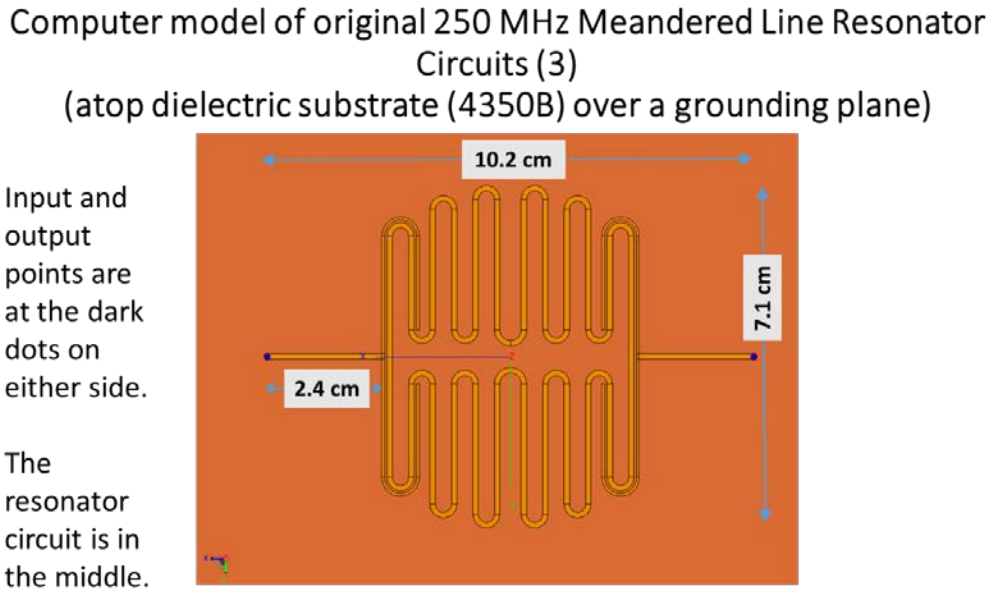

Fig. 1 FEKO top view of original 250-MHz meandered-line resonator circuits

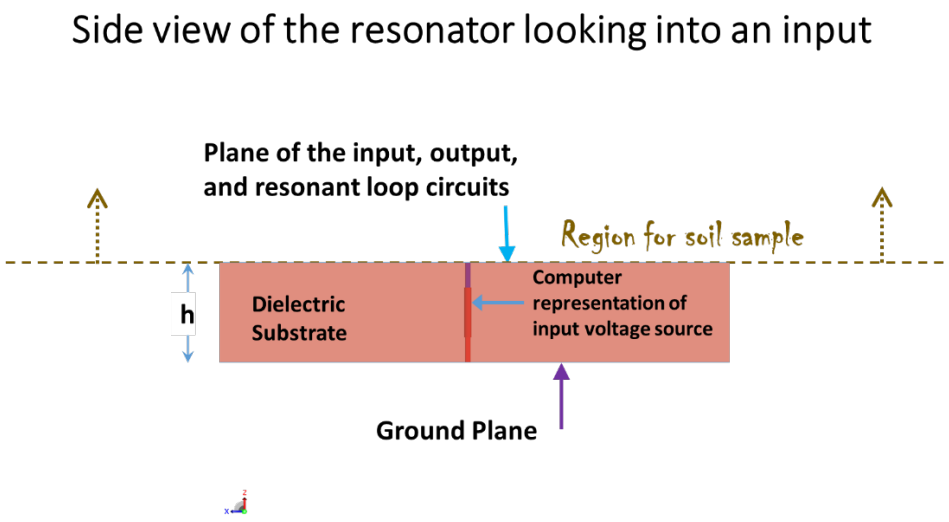

Fig. 2 View from port into resonator model

Three primary constraints on the resonator design were necessary to render the resonator practical and useful. First, the input and output lines and the resonator circuit line needed to have input impedances of approximately 50 Ω. Secondly, the size of the sensor should not be too large since a larger sensor is harder to handle and more difficult to make uniform contact with the soil. Lastly, F_o should be as low as 25 to 40 MHz so that the low end of the 20- to 90-MHz band would be included. The resonance frequencies should not be so low that resonances shifted lower by soil loading would be cut off by the 20-MHz limit.

Usually higher-order resonances also appear and are important for accumulating data over a band and improving statistics of what is probably somewhat noisy data. High-end frequencies could be covered by a second resonator specifically designed to cover only the high end. However, if F_o of a resonator was too close to 90 MHz, only one resonance might be able to participate in the sensing. Such a circumstance would reduce the advantage of the case in which a few resonances showed up just below 90 MHz, allowing more data to become available within the same measurement run.

Since resonances occur at resonator ring lengths that are integer multiples of the guided wavelength, λ_g, one way to move to lower frequencies would be to increase the resonant loop line length. To increase the line length while minimizing the areal footprint of the sensor, more meanders were added. Mazzaro[1] guides us by describing the goal as maximizing the length-to-enclosed area ratio. However, the dielectric constant of the substrate was also important in tuning for lower resonant frequencies while maintaining a reasonable footprint for the device. A higher dielectric constant would tend to render the sensor electromagnetically larger with the same physical size so that it would resonate at lower frequencies. The first resonant frequency is then

$$\boldsymbol{F_0 = \frac{v}{\lambda_g} = \frac{c}{\lambda_g \sqrt{|\varepsilon_{\text{eff}}|}}}, \tag{1}$$

where c is the speed of light, v is the speed of light in the medium, λ_g, is the micro-strip guided wavelength, and ε_{eff} is the effective permittivity of the medium. By the earlier guidance, we needed to increase the line length-to-area enclosed ratio, but by Eq. 1 a reduction in the resonance frequencies occurs with an increase in $|\varepsilon_{\text{eff}}|$. The medium, in effect, consists of a combination of soil or air on the "top" of the resonator as shown in Fig. 2 and a dielectric substrate of a limited thickness, h. An unloaded resonator has just air above the resonator as shown in the figure, whereas a loaded resonator would have soil there instead. The difference in the net medium when changing from air to soil loading produces the changes in the resonances that facilitate permittivity measurement.

In order to maintain the impedance of the strip lines and circuits at 50 Ω, the same set of equations that are found in Mazzaro's report[1] were used:

$$Z_0 = \frac{Z_0^{air}}{\sqrt{|\varepsilon_{eff}|}}. \tag{2}$$

$$Z_0^{air} = 60 ln\left[\frac{F_1 h}{w} + \sqrt{1 + \left(\frac{2h}{w}\right)^2}\right]. \tag{3}$$

$$F_1 = 6 + (2\pi - 6)exp\left\{-\left(31h/_W\right)^{0.7528}\right\}. \quad (4)$$

$$\left|\varepsilon_{eff}\right| = \frac{\varepsilon_r+1}{2} + \left(\frac{\varepsilon_r-1}{2}\right)\left(1 + \frac{10h}{w}\right)^{-a\cdot b}. \quad (5)$$

$$a = \frac{1}{49} ln\left[\frac{(w/h)^4 + \{w/(52h)\}^2}{(w/h)^4 + 0.432}\right] + \frac{10}{187} ln\left[1 + \left(\frac{10w}{181h}\right)^3\right]. \quad (6)$$

$$b = 0.564\left[\frac{\varepsilon_r - 0.9}{\varepsilon_r + 3}\right]^{0.053}. \quad (7)$$

Here, Z_0 is the line impedance, ε_r is the dielectric constant of the substrate, h is the height or thickness of the substrate, and w is the line width. For a given h and ε_r, Z_0 is plotted against w to find what the latter needs to be so that $Z_0 \approx 50\ \Omega$. The height and dielectric can also be modified in an effort to produce lower resonant frequencies.

In an exception to line widths as computed using Eqs. 2–7, in Mazzaro's model[1] and ours, widths of the parts of the input and output lines next to and conformal with the resonator circuit were *w/2*. Mazzaro had explored a range of separation gap widths between the I/O lines and the resonator circuit to optimize coupling and resonance Q's and then settled on *w/2*. Our models continued with gap widths of *w/2*.

In this computer modeling study, only permittivity and thickness characteristics of Rogers Corporation laminates[3,4] were used. The use of possible laminate thicknesses that could be created through mutually bonded layers of their laminates were also explored. Rogers RO4350B was originally considered (which was the dielectric used in the original 250-MHz resonator). However, it soon became clear that a laminate with the highest dielectric value, RO3010, produced far better resonances and kept the sensor footprint lowest. For those reasons, in pursuit of our goal, only RO3010 was used for further modeling of the sensor. Consequently, modeling for RO4350B and RO3010 (hereafter referred to as 4350 and 3010) are the only dielectrics considered in this report.

Measured permittivities for Yuma, Arizona, soils[5] containing 2.5%, 5%, 10%, and 15% water (H_2O) were used for computational simulations of the new models; the values used were from a measurement taken at 50 MHz. Simulations of the 250-MHz model used permittivities taken at 250 MHz.

3. Results

3.1 Design Results

Figure 3 shows the S_{21} parameter response for the original 250-MHz meandered-line ring-resonator with and without Yuma, Arizona, soil composed of 2.5% H_2O as a baseline. The reduction in the resonance frequency and the resonance Q with the soil load is plainly evident.

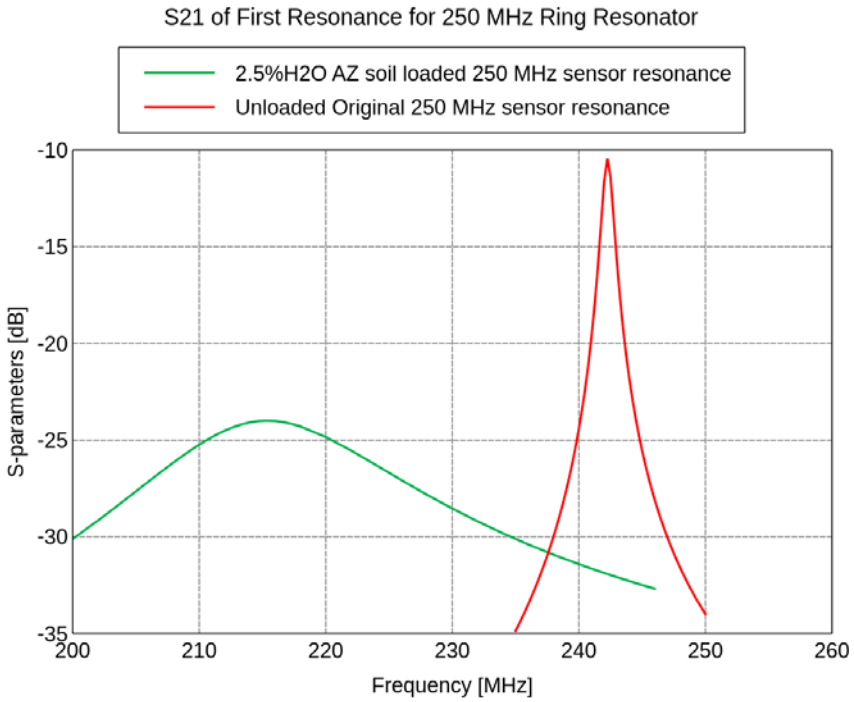

Fig. 3 Loaded and unloaded F_0 for original meandered-line resonator

A new resonator array (M5) was created in which the length of the loops was increased and the number of loops was doubled from the original resonator to lower the frequency of the first resonance, F_0. The substrate thickness was fixed at 0.64 mm, but simulated with 4350B substrate and then again with 3010, which have real dielectric constants at 3.66 and 11.2, respectively. Using the conditions to set the line width in each model such that its impedance is 50 Ω results in line widths of 1.4 and 0.53 mm, respectively, which was done by scaling the model shown in Fig. 4. The M5 model with the 3010 substrate is more than 2.6 times smaller per dimension than the model using the 4350 substrate.

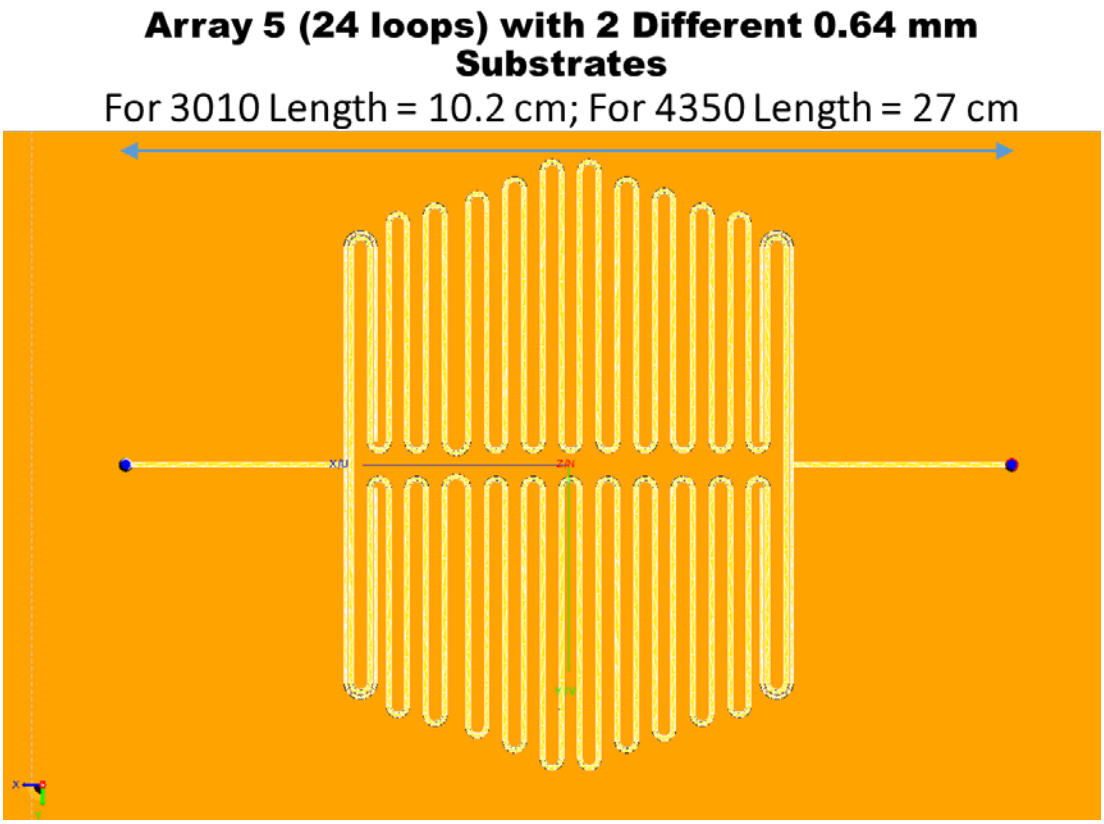

Fig. 4 Comparing sizes for model 5 using 3010 and 4350 substrates

Figure 5 shows the resultant S_{21} parameter over frequency for the two Array 5 models. The smaller version using the 3010 substrate shows F_0 to be substantially lower in frequency, at about 77 MHz, compared to the 4350 substrate at about 95 MHz, and its magnitude is more than 10 dB higher. The poorer resonance performance here and in other models, along with the much larger size of the 4350 substrate sensors, directed our further efforts toward exclusive use of the 3010 substrate.

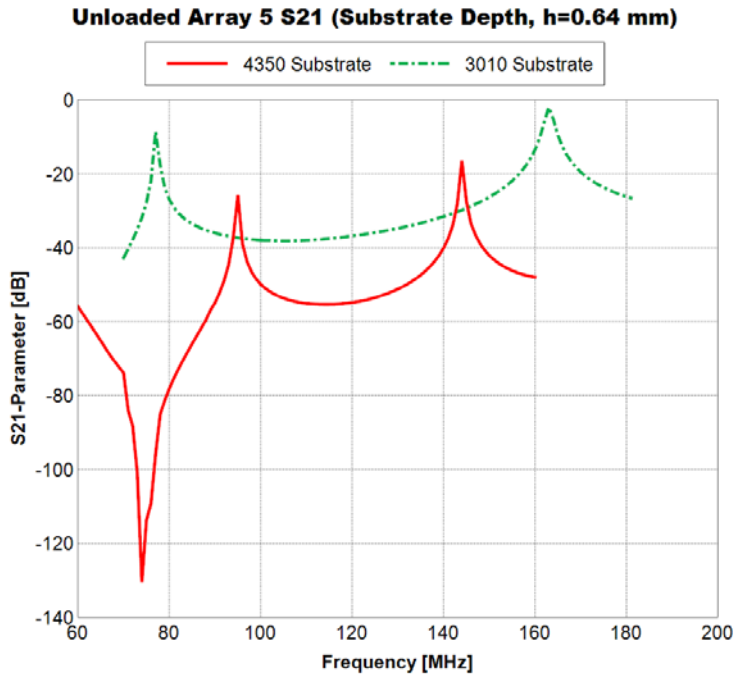

Fig. 5 Comparison of S_{21} parameters for Array 5 with 4350 and 3010 substrates

With the assumption that in order to produce a ring resonator that can operate at even lower frequencies, an increase in the meander line length was needed, we created a new computer model, Array 7. Array 7 doubled the number of loops to 48 and lengthened the loops by over four times. This line length increase was unsuccessful as F_0 was still stuck at 77 MHz. Other changes in the geometry of the lines did not improve the result.

The next possibility was to increase the substrate thickness. When we doubled the 3010 substrate thickness to 1.28 mm for Array 7, F_0 dropped down to 37 MHz, almost half of 77 MHz. Array 7 with the 1.28-mm substrate is shown in Fig. 6.

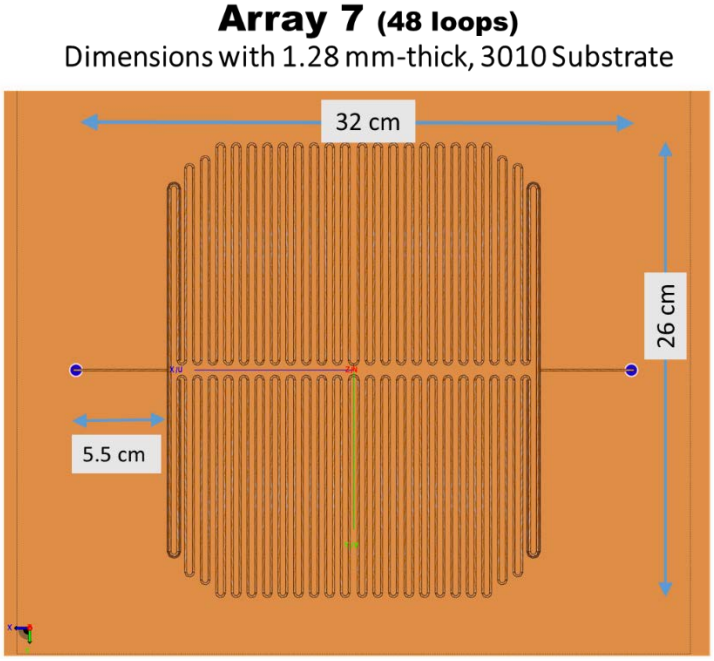

Fig. 6 Array 7 with 1.28-mm-thick 3010 substrate

The sensor was loaded with the different Arizona soils using measured permittivities at 50 MHz in the computations except for case of Eglin soil that used 100-MHz permittivities.[6] Figure 7 shows the S_{21} for the unloaded Array 7 and for loading with five different soils over the frequency range of 20 to 70 MHz. Sparse frequency sampling for the computations on some of the curves is the reason for the lack of smoothness on those curves. While the real part of the permittivity is determined from the shift in the resonance frequency, the imaginary part comes largely from the change in the inverse Q of the resonance. The resonance must be over 3 dB in magnitude to determine the Q since the definition refers to the width at 3 dB down from the peak. For the Arizona soils in Fig. 7, as the H_2O content increases, the number of resonances usable for measurement of Q decreases so that only the drier soils have a few or several useful resonances with this sensor. At 10% and 15% H_2O content, only one resonance may be available. A rather different soil type, such as the apparently less lossy Eglin soil, may be much more easily measured over a wider frequency band all at once.

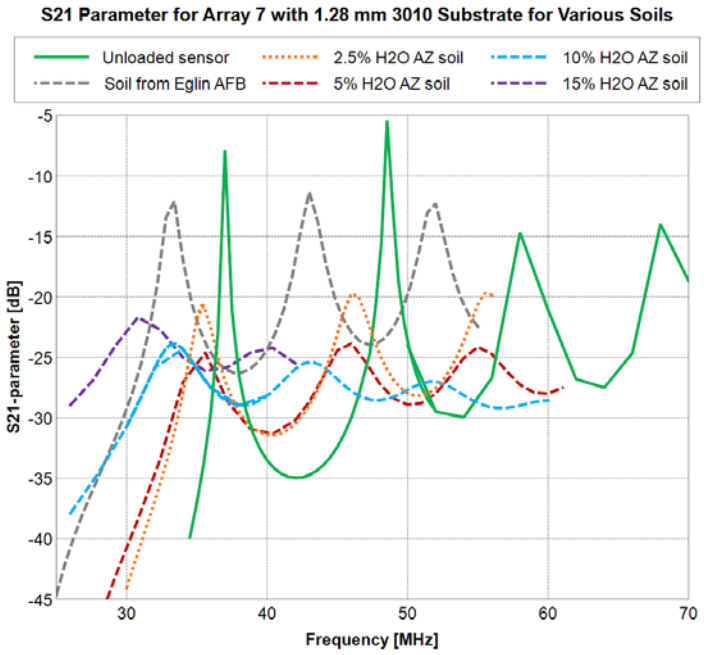

Fig. 7 S_{21} parameter for Array 7 unloaded and loaded with soils

The meander line was lengthened in Array 7 by adding more loops (from 48 to 60). However, F_0 did not drop but remained at 37 MHz. When the substrate thickness was increased to 1.53 mm, the resonance dropped to 31 MHz. This became our Model 7yy as shown in Fig. 8. The S_{21} responses for the unloaded sensors are shown in Fig. 9 along with soil loaded on the 1.53-mm substrate sensor. Since the substrate was thickened, line widths had to be increased to provide a 50-Ω line impedance, so that the 60-loop model with the 1.53-mm substrate (Array 7yy) was larger than 60-loop model with the 1.28-mm substrate. The results of Fig. 9 further indicated that a thicker substrate is key to bringing down the resonance frequency.

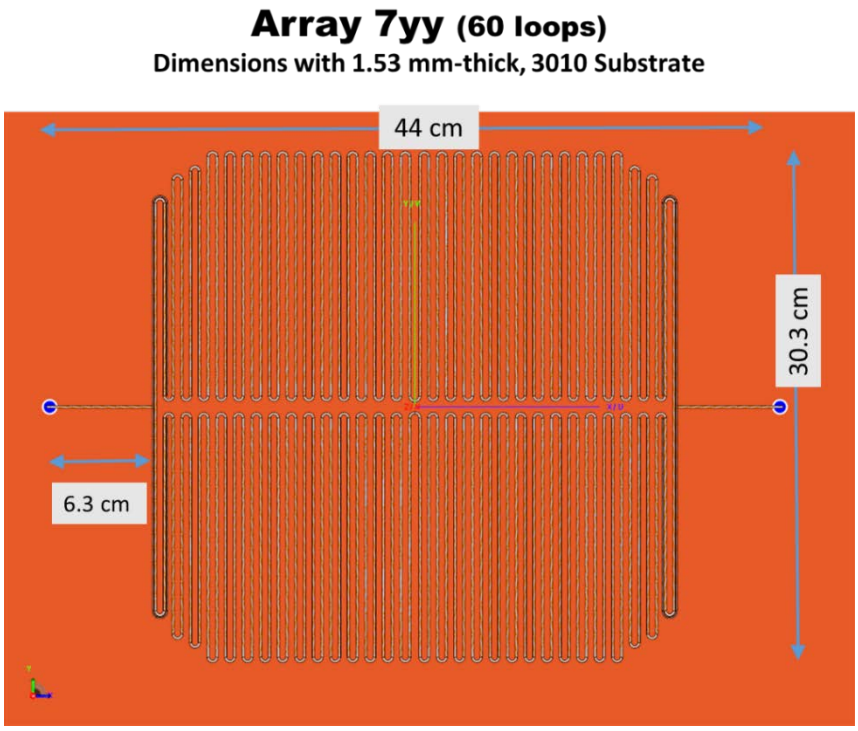

Fig. 8 Array 7yy with 1.53-mm-thick 3010 substrate and 60 loops

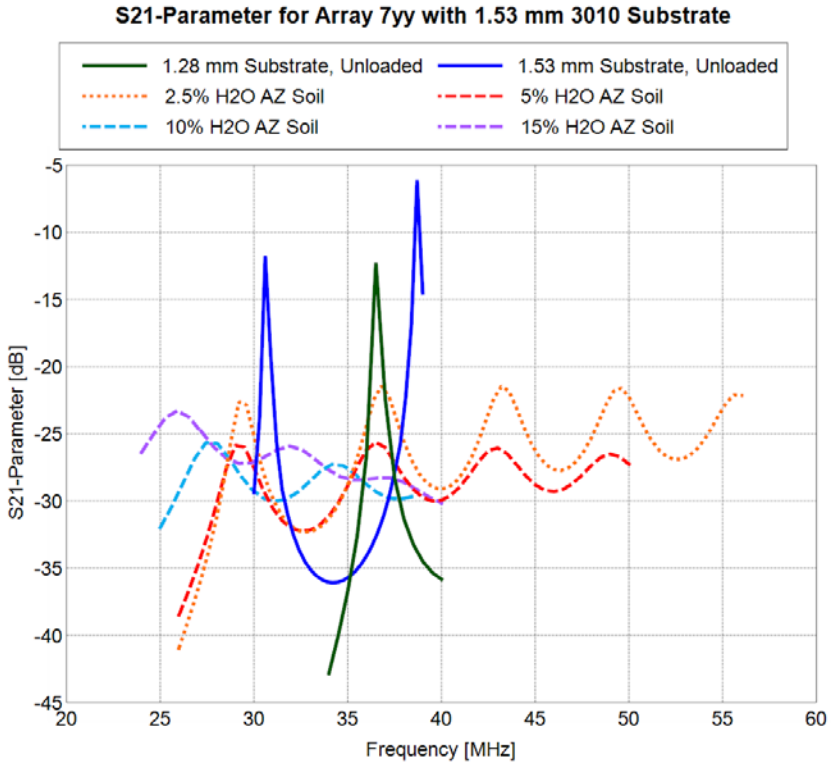

Fig. 9 S_{21} parameter for Array 7yy with and without soils compared with the scaled smaller 1.28-mm substrate version without soil

In pursuit of still lower resonance frequencies we again increase the substrate thickness and resonator line length by adding more loops. Array 7zy with 72 loops and a 1.92-mm-thick 3010 substrate is shown in Fig. 10 and its S_{21} parameter response versus frequency is shown in Fig. 11. Array 7zz with 84 loops and a 1.92-mm-thick 3010 substrate is shown in Fig. 12 and its S_{21} parameter response versus frequency is shown in Fig. 13. That F_0 is 24 MHz for both 7zy and 7zz is evidence that increases merely in the meander line length are not sufficient to lower F_0.

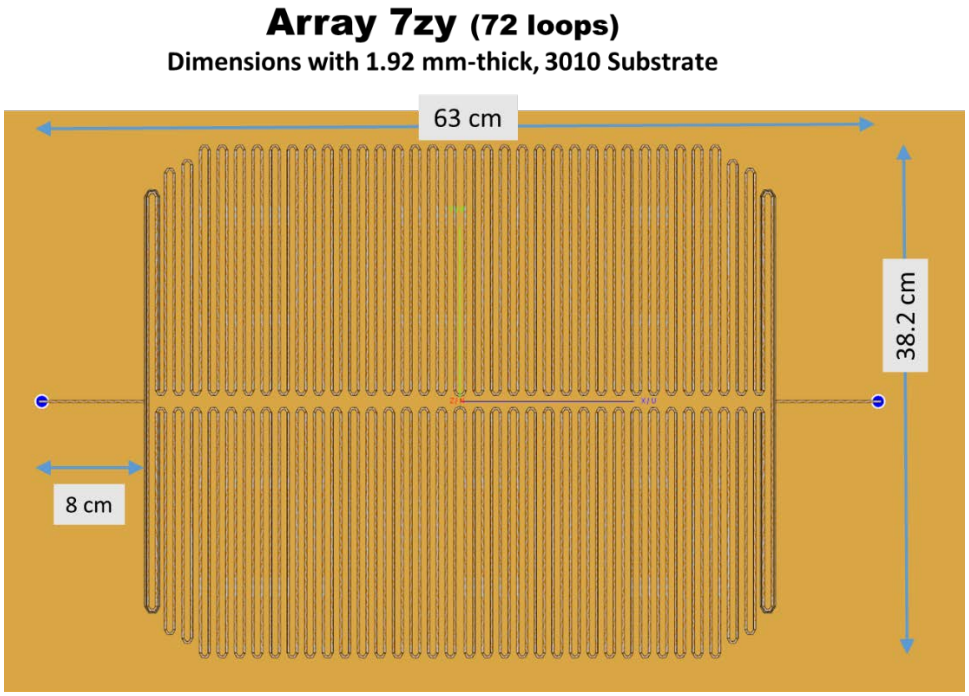

Fig. 10 Array 7zy with 72 loops and 1.92-mm substrate

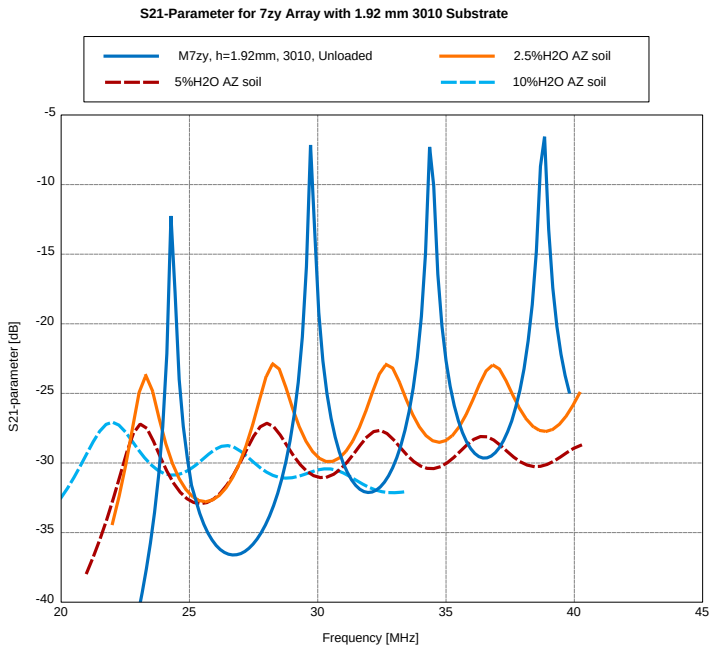

Fig. 11 S_{21} parameter versus frequency for Array 7zy

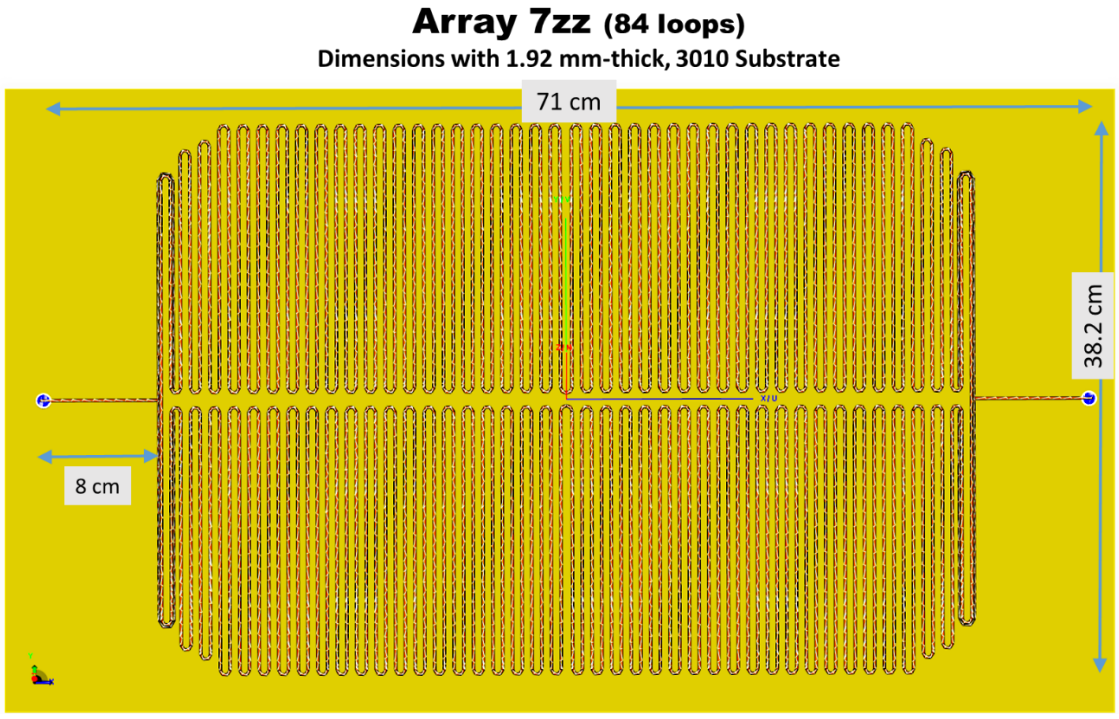

Fig. 12 Array 7zz with 84 loops and 1.92-mm substrate

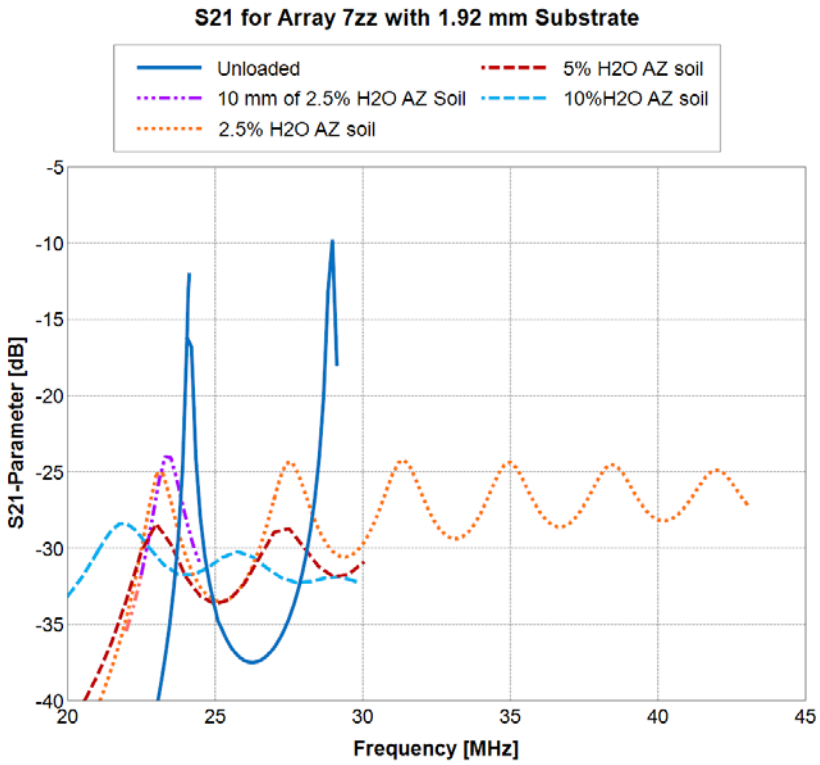

Fig. 13 S_{21} parameter versus frequency for Array 7zz

The sequence of S_{21} graphs from Array 7 through 7yy, 7zy, and 7zz show that the peaks for soil-loaded sensors decline in magnitude and the frequency separations between resonances also shorten. This behavior trend is a measure of slightly poorer performance, possibly due to increased radiated losses from the increasing number of loops. The latter behavior indicates that the resonances that are available consequently measure over a narrower frequency range, so that additional sensors tuned to other frequencies would be needed to span the entire 20- to 90-MHz band.

The success in lowering the frequencies of the resonances by thickening the substrate rather than by increasing the meander line length pointed to new possibilities in the resonator design. Following this new guidance inferred from the modeling, we now remodeled some of the earlier fewer-loop models with thicker substrates. These new models were likely to be smaller in size than the 7yy, 7zy, and 7zz models that were undesirably large.

Model 7xxy has the same shape as Model 7 (M7), but its substrate has increased to 1.53 mm from the 1.28 mm M7 has. Therefore, by the impedance condition on its strip lines, its line width has increased to 1.33 mm from 1.09 mm, as has its whole model size by the same proportion. This made it larger than M7, but smaller than 7yy while its F_0 came at 31 MHz, the same as 7yy, as shown in Fig. 14.

Additionally, its soil-loaded resonance peaks are 2 or 3 dB higher and the dynamic range of the resonances (peak to trough) is slightly greater than 7yy.

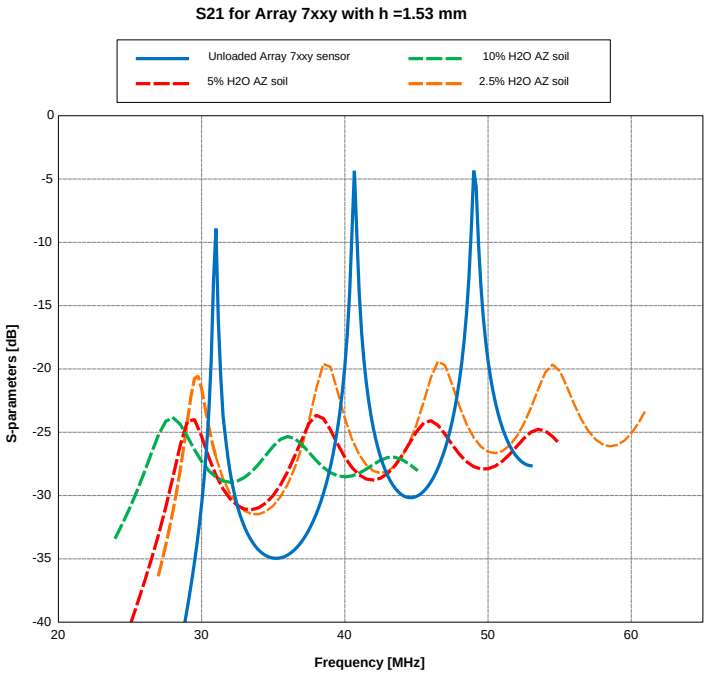

Fig. 14 S_{21} for Array 7xxy with and without soil

Model 6 is similar to Model 7, but with only 32 loops as shown in Fig. 15. Specifically, M6u has a 1.72-mm substrate and M6zz has a 1.92-mm substrate. Fig. 16 shows the S_{21} for both of these models with and without soil. For M6zz, F_0 was at 29 MHz and for M6u it was at about 32.7 MHz.

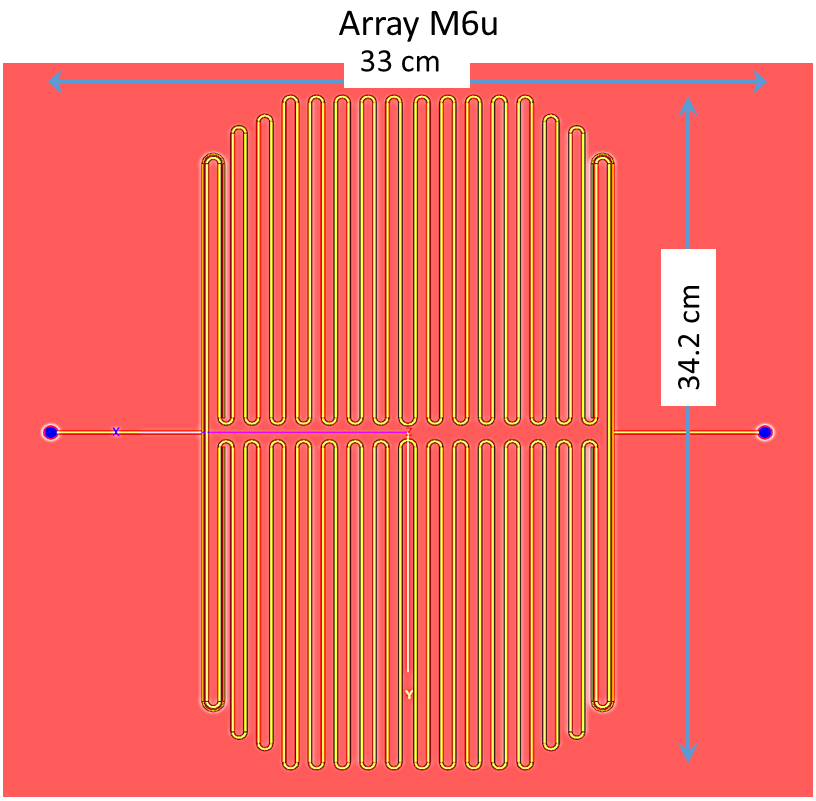

Fig. 15 Array M6zz

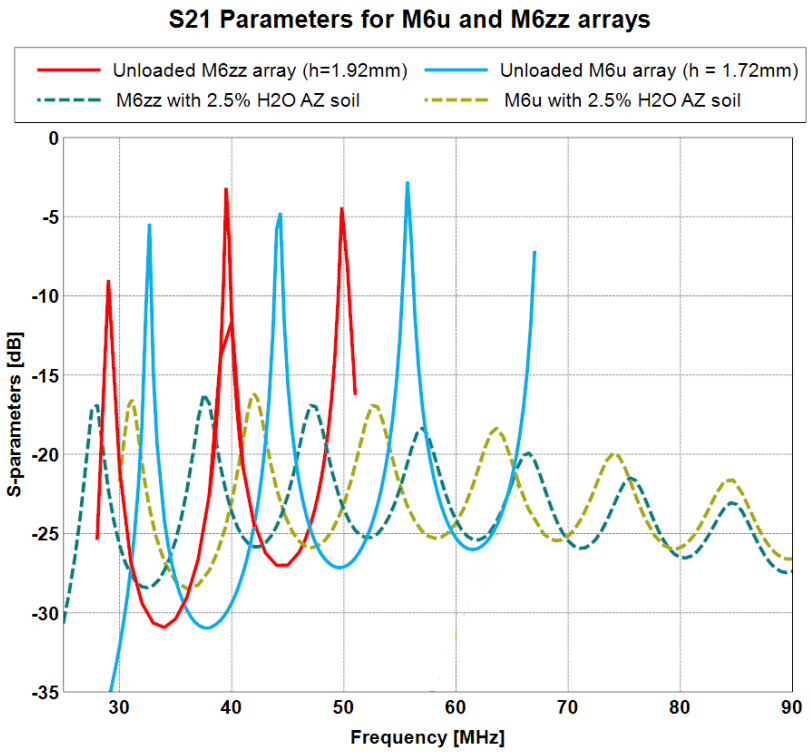

Fig. 16 S_{21} for Arrays M6u and M6zz

Variants of the 24-loop M5 were also developed, with 3010 substrate thicknesses of 1.53, 1.72, and 1.92 mm for Arrays M5yy, M5u, and M5zz, respectively. Array M5u is shown in Fig. 17. The unloaded F_0's of these same three arrays are respectively 31, 27.5, and 24.6 MHz, as can be seen in the S_{21} curves of Fig. 18. These M5 variants are distinguished by their small size combined with the ability to reach to the lowest frequencies we need. Figure 19 shows the S_{21} for M5u with and without several soils. These M5 variants all cover the 20- to 90-MHz range well, but among all of the M5 models we evaluated, M5u had the best ability to cover the entire 20- to 90-MHz band over the four different H_2O content soils. Furthermore, as seen in Table 1, M5u is considerably smaller in size from the largest models and is approximately the same size as the early M5-4350h64 model that could not even penetrate into the 20- to 90-MHz range.

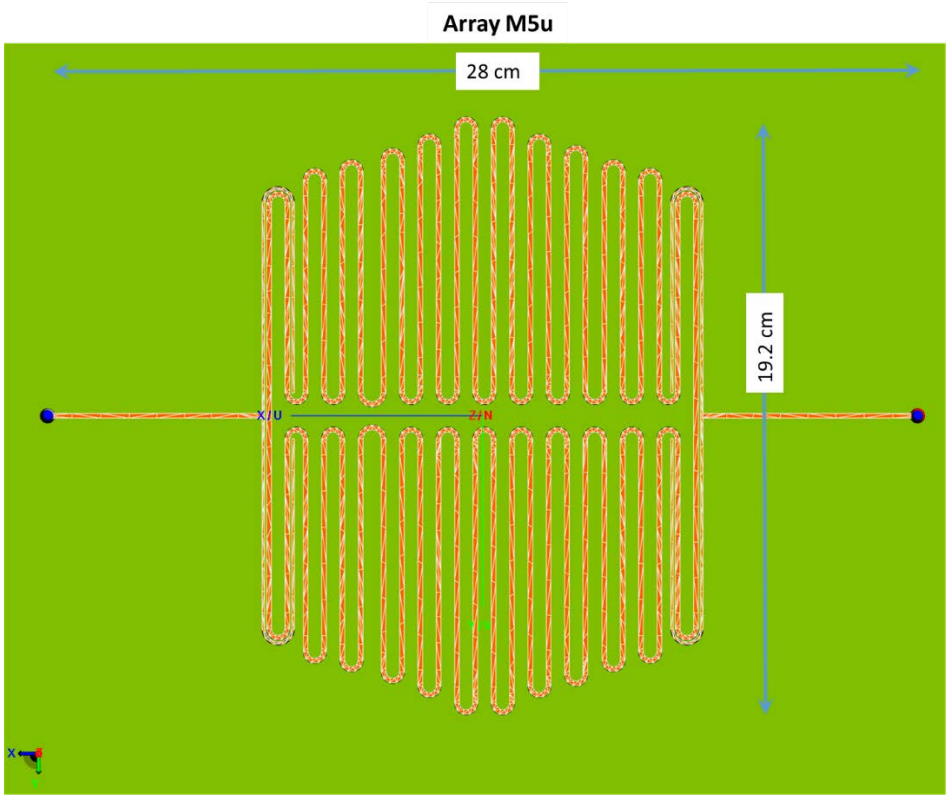

Fig. 17 Array M5u

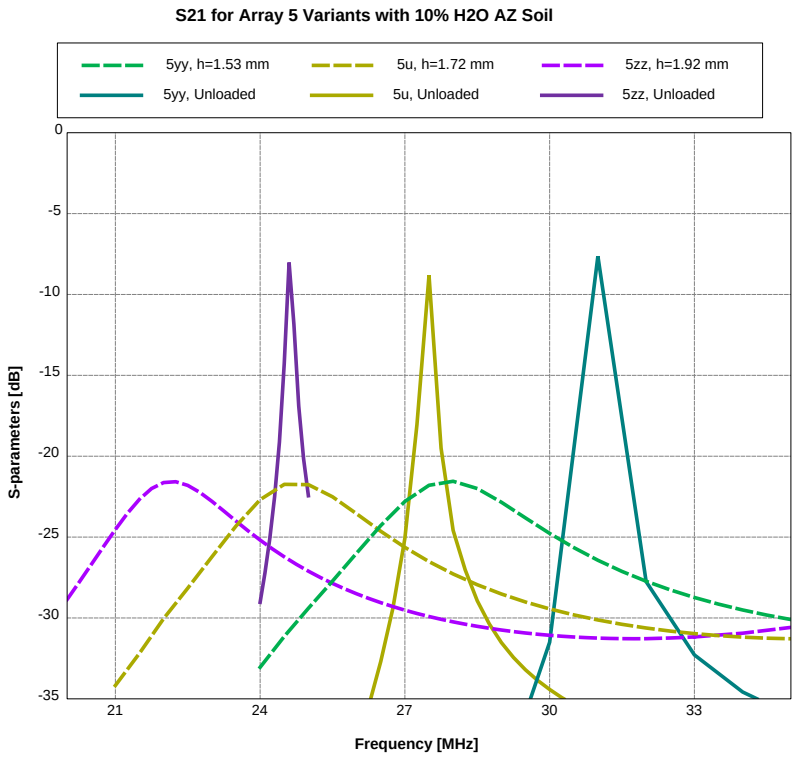

Fig. 18 S_{21} for Arrays M5yy, M5u, and M5zz with and without 10% H_2O Arizona soil

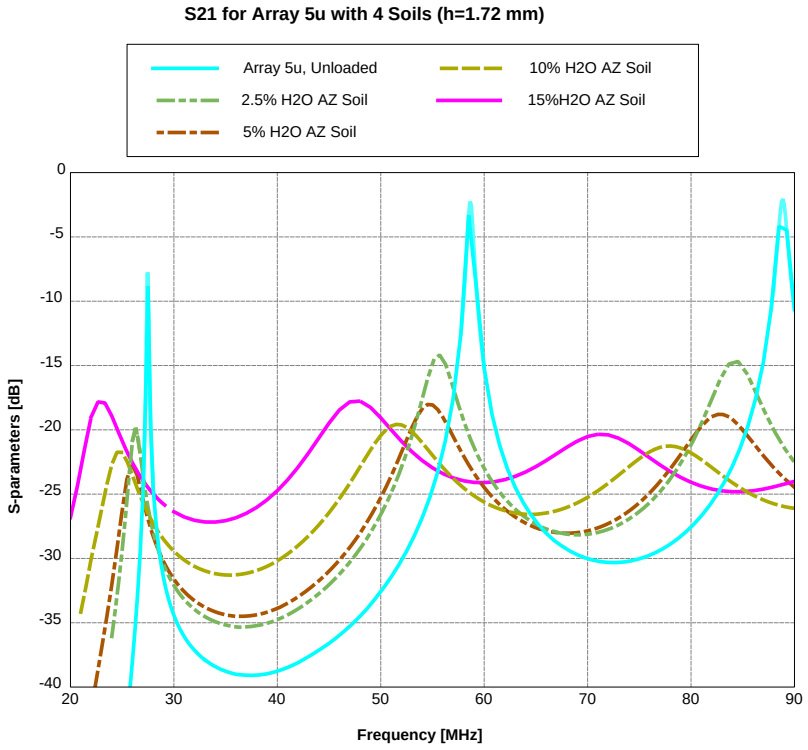

Fig. 19 S_{21} for Array M5u with four soils and without soil over 20 to 90 MHz

Table 1 Summary of model characteristics and results

Model	Length (T to T) X width (cm)	Lead length (cm)	No. loops	Substrate thickness h (mm)	Line width (mm)	Substrate ε_r	Substrate tan δ	Unloaded F_0 (MHz)	Resonance separation (MHz)	Comments likely usable resonances for soils with 2.5% H_2O; 5% H_2O; 10% H_2O; 15% H_2O, respectively
250 MHz	10.2 × 7.1	2.4	12	0.508	1.11	3.66	0.0037	242	. . .	Original resonator
M5-4350 h64	26.8 × 18.3	6.7	24	0.64	1.4	3.66	0.0037	91	48	. . .
M5-3010 h64	10.2 × 7	2.5	24	0.64	0.53	11.2	0.0022	77	86	. . .
M5yy	25 × 17	6.2	24	1.53	1.3	11.2	0.0022	31	26–28	2; 2; 2
M5u	28 × 19.2	7	24	1.72	1.465	11.2	0.0022	27.5	30–31	3; 3; 3; 3
M5zz	31.3 × 21.3	7.8	24	1.92	1.635	11.2	0.0022	24.6	35	3; 3; 3; 1
M6u	33 × 34.2	7.1	32	1.72	1.465	11.2	0.0022	32.7	11	6; 3; 2; 1
M6zz	36.7 × 38.2	8	32	1.92	1.635	11.2	0.0022	29	10	7; 3; 2; 1
M7	31 × 26	5.5	48	1.28	1.09	11.2	0.0022	37	10	6; 2, 1, 1
M7xxy	37.4 × 30.5	6.3	48	1.53	1.3	11.2	0.0022	31	8–9	5; 2; 1; 1
M7yy	44 × 30.3	6.3	60	1.53	1.3	11.2	0.0022	31	8	5; 2; 1
M7zy	63 × 38.2	8	72	1.92	1.635	11.2	0.0022	24	5	4; 2; 1
M7zz	71 × 38.2	8	84	1.92	1.635	11.2	0.0022	24	3–4	4; 1

Table 1 both characterizes our resonator models and summarizes important results from our computer experiments to lower the resonance frequencies in the models. Results such as resonance separations are approximate as they tend to vary over the band. Soil-loaded resonances vary from a few to several megahertz below their respective unloaded sensor resonances, and that frequency depression increases with increasing frequency within the band. Consequently, separations between soil-loaded resonances tend to be slightly less than resonances from unloaded sensors.

In the drive toward reaching an F_0 that lies as low as the 20-MHz decade, the strength of the soil-loaded signals in some models decreased so much so that higher-order resonances, particularly for moister soils, became unusable. In these cases the sensor can provide data for about only one or a few decades of megahertz near F_0 and none for the high end of our band as shown in Table 2.

Table 2 Performance comparisons among the models

Model	Approx. size with leads (cm)	Advantages	Disadvantages
M5 4350	27 × 18	. . .	Does not reach into range
M5 3010	10 × 7	Small (footprint)	Only F_0 in range and only at top of range
M5yy	25 × 17	Small; good coverage of moist soil	Only F_0 and F_1 within target range
M5u	28 × 19.2	Small; three resonances for most soils span the entire range; strong signals; coverage for moist soils very good	Sparse coverage for narrow frequency band since resonances are spread apart
M5zz	31.3 × 21.3	Almost as good as M5u, just slightly larger footprint; more tolerance for grainy soil	Resonances spread slightly further apart than M5u
M6u	33 × 34.2	Excellent for dry soils; good for moist	F_0 only down to 32.7 MHz
M6zz	36.7 × 38.2	Excellent for dry soils; good for moist; more tolerance for grainy soil	. . .
M7	32 × 26	First five resonances within range; strong soil response	F_0 only down to 37 MHz
M7xxy	37.4 × 30.5	Good strength for dry soil	F_0 only down to 31 MHz; does not cover upper part of band
M7yy	44 × 30	F_0 at 31 MHz; six resonances in band for dry soil up to 60 MHz	Covers only low end of band for moist soils; only F_0 for 10% H_2O or moister soil

Table 2 Performance comparisons among the models (continued)

Model	Approx. size with leads (cm)	Advantages	Disadvantages
M7zy	63 × 38	F_0 at 24 MHz; resonances 5 MHz apart makes for good frequency resolution; more tolerance for grainy soil	Big; covers only low end of band; poor coverage for moist soils; close resonances may interfere with Q measurement
M7zz	71 × 38	F_0 at 24 MHz; resonances 5 MHz apart makes for good frequency resolution; more tolerance for grainy soil	Big; covers only lower 14-MHz range of band for dry soil; little or none for moist soil; close resonances

If models with the same substrate thickness are compared, we find that merely adding more length to the resonator does not necessarily contribute to the goal of reducing the frequency. For example, in the case of M7zy to M7zz, or M7xxy to M7yy, no improvement occurs. Even the comparison of M5yy to the latter pair shows no difference. It appears that the substrate thickness is the determining factor of the minimum resonance frequency, perhaps by setting a lower bound on it.

A constraint that the line widths, *w*, are set so that line impedances are related to the substrate thickness through Eqs. 2–7 exists. It turns out that *w* is nearly linearly related to *h* for our problem set. An increase in *h*, leads to an increase in *w* so the model must scale the size of models with a higher *h* so that *w* is correct, as has been our design approach. If we compare F_0 for models that are scaled by these relations, we find the resultant frequencies appear to have a lower bound on the F_0, which scales linearly with h^{-1} and w^{-1} as shown in Figs. 20 and 21. Most of the results actually fall on, or very near to, this bounding line. Possibly the linear fit of the bound to w^{-1} is slightly better as we see in the case of M5-3010h64 to M7, but the differences are too close to tell which might be the driver. For F_0 occurrences somewhat above the bounding line, the geometry of the circuits may not be well suited to the task of minimizing the frequency. One such occurrence is the test case modification of the original 250-MHz resonator with its substrate replaced by 1.92-mm-thick 3010 substrate shown as M250 in Figs. 20 and 21. M250 is only able to bring F_0 down to 105.8 MHz.

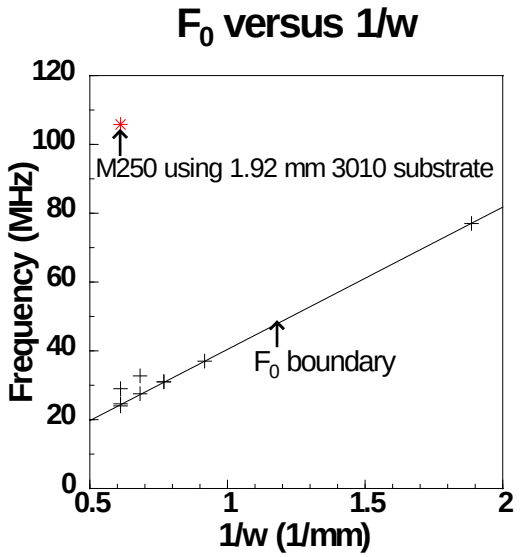

Fig. 20 $F_0 \geq 41.4\ w^{-1} - 0.98$

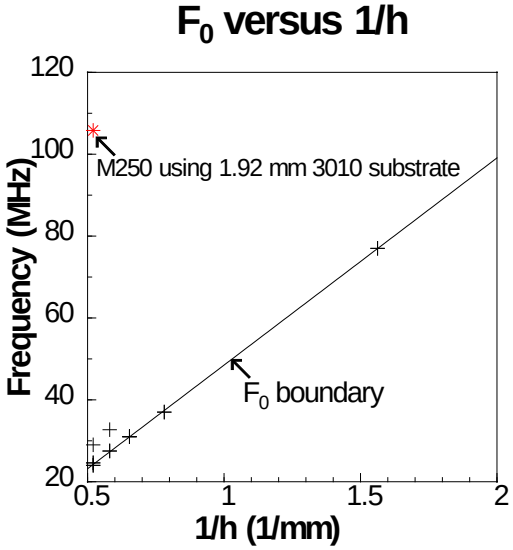

Fig. 21 $F_0 \geq 50.6\ h^{-1} - 2.14$

Checking for other features of our models that scale with *w*, we note that the gap between the lead lines and the resonator is *w/2* in our models. Also, the length of the lead lines directed away from the resonator is also proportional to *w* in our models. Yet, when either the gap distance or lead line length was changed, the resonant frequency did not change so it is apparent they do not affect the resonant frequency.

Table 2 compares the performances of the different models. Several factors play a role in the suitability for the task: how well the 20- to 90-MHz band is covered; the strength of the signal in terms of the "absolute" peak; the resonance height from the trough; the ability to respond to different soils; and the sensor size.

Every model has advantages and disadvantages. One major advantage for models with short separation between resonances and multiple resonances for a particular soil is that they can provide a lot of data in a narrow frequency band so that the permittivity can be more easily evaluated for a particular frequency rather than an average for wide band. The major disadvantage is that another sensor would be needed to cover another part of the band. In the reverse case, a sensor with strong widely separated resonances can quickly yield an average for the whole band but just provide limited samples at narrow spots in the band.

For sensors with larger *w*, gaps and holes or enclosures would be larger as well as conductive contact surfaces for the soil. In consideration of these characteristics, it is possible that sensors with a larger *w* would be less sensitive to the grainy character of the soil. Grains would be relatively smaller to the sensor surfaces so there would be more contacts with the soil and more microcircuit pathways within the soil and to the sensor surface; the soil would effectively act more homogeneous. If we compare some of our *w*'s at 1.635 mm with the original and earlier sensors at 1.11 mm, we see they are nearly 50% wider. To what extent a sensor with $w = 1.635$ mm reduces signal noise or error awaits tests with physical experiments.

The Arizona soil we used with different soil moistures may be especially challenging among soil types[7] or simply lossy. Most model resonances were poor at H_2O contents of 10%–15%. For most they could produce only one or two resonances at these frequencies. This means that in the top range of the band no data would be available for those moisture levels since the separation between resonances was usually around 10 MHz or less. In that case, an auxiliary higher frequency sensor would need to be designed to cover the top half of the range. Especially for the largest sensors, responses even for dry soil at 2.5% H_2O would probably be unable to adequately respond in the top 20 or 30 MHz of the band. For example with M7yy and 2.5% H_2O soil, F_0 would be at about 29 MHz with resonance separation at 8 MHz, so that a final usable resonance would be at $29 + 4 \times 8 = 61$ MHz.

3.2. Sufficient Sample Depths for Operation

In order to measure soil permittivity a layer of soil must be in firm and uniform contact with the circuit side of the sensor. This is usually accomplished by facing the circuit side, or "face side", down against the ground with the ground being very

flat to maximize contact with the soil. However, there are times when only a sample of soil is available to measure. In this case the soil sample of limited volume would have a limited depth against the face of the sensor, which would almost certainly need to face up into the air. The question then arises as to what depth of soil is sufficient for the sensor to properly characterize the permittivity of the soil against it. If the depth is too small, then the sensor is measuring the properties of the soil and air above combined, resulting in an error or value different from the true permittivity of the soil. As we discuss later in this section, a nonlinear effect also renders use of small soil depths as unreliable. The sensor will need to be calibrated against some dielectric standards. Such a standard will also need to be of sufficient depth or thickness so that the calibration itself will not be in error.

For simulations of resonances for varied soil depths, we have again used the known soil permittivities from Carin et al.,[5] at 50 MHz for the low-frequency sensor and at 250 MHz for the high-frequency 250-MHz sensor, to approximate the actual soil permittivities at the actual resonance frequencies occurring in the simulations. In this section, we show results of simulations of various depths of uniform soil against the face of the sensor compared with the case of an unlimited depth of uniform dielectric against the sensor face. The closer the two cases agree, the more certain the user can be that such a depth is adequate to properly measure the permittivity of the soil.

Alternatively, there is more than one way to assess adequate agreement. We can graphically compare S_{21} resonance curves of sensors loaded with several different depths for two different soils, as shown in Figs. 22–27. The ruler superimposed on these six figures is meant to give a measure of degree of agreement in percent between the unlimited soil depth, as the ideal, and curves representing the limited depths. For example, in Fig. 22, 2 mm of soil depth gives 74% agreement while 25 mm depth gives about 99%.

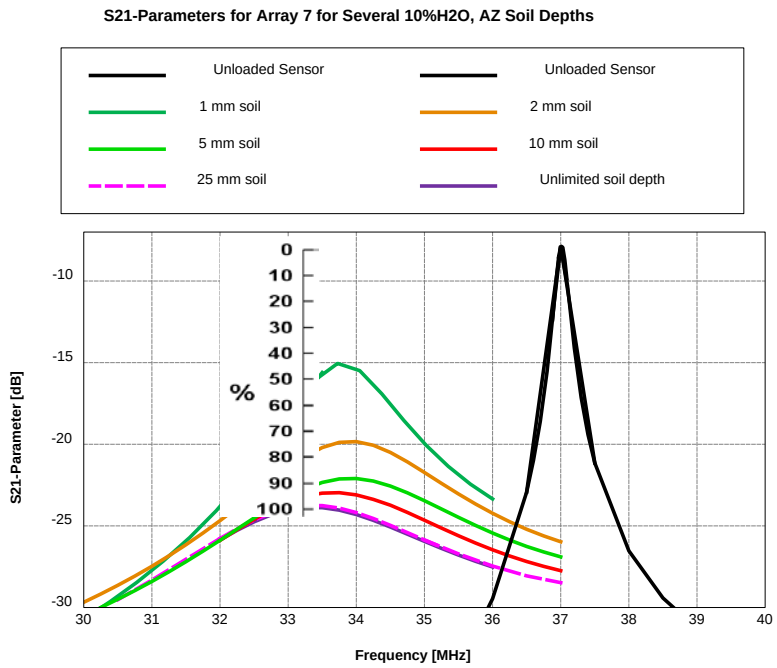

Fig. 22 Resonances for M7 with several 10% H_2O Arizona soil depths

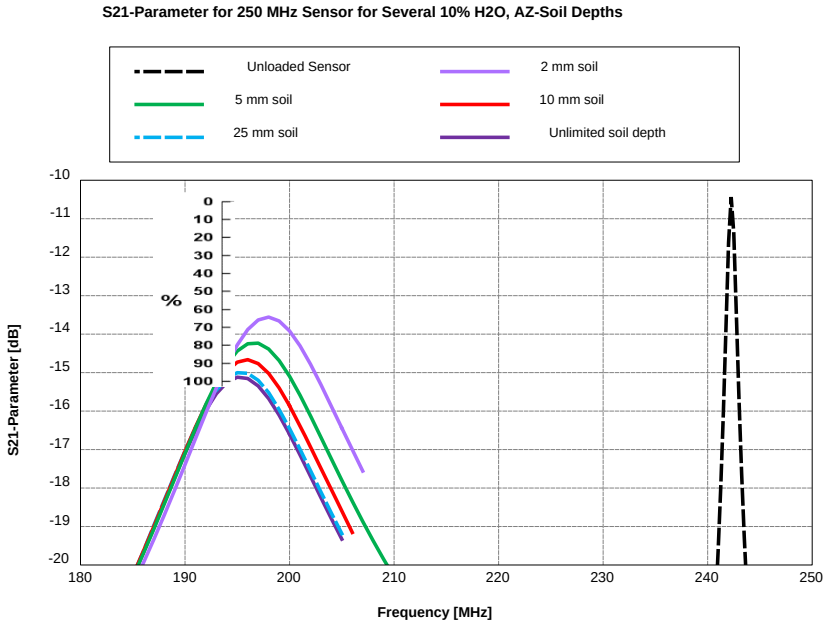

Fig. 23 Resonances for M250 with several 10% H_2O Arizona soil depths

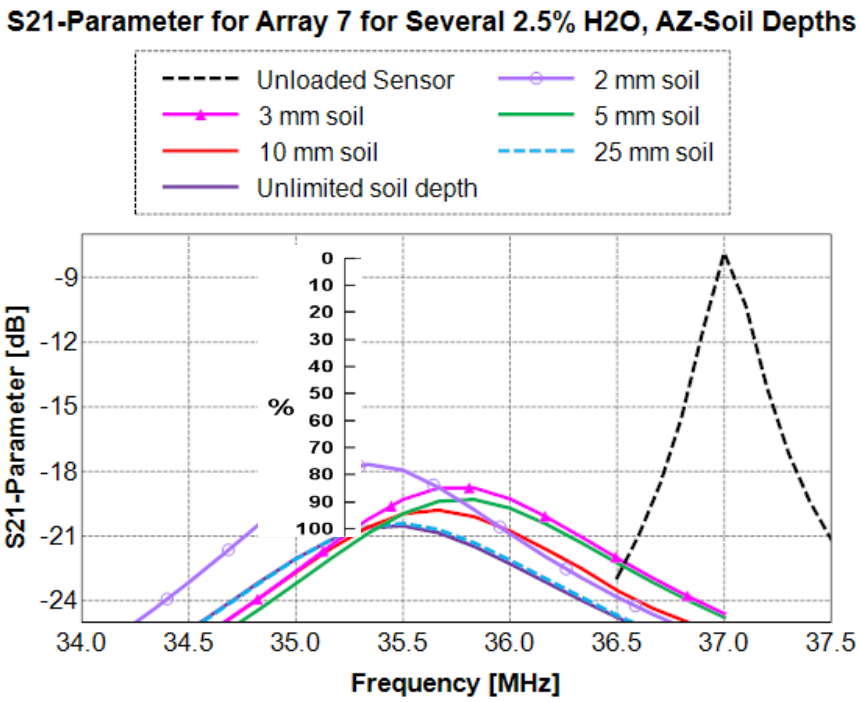

Fig. 24 Resonances for M7 with several 2.5% H_2O Arizona soil depths

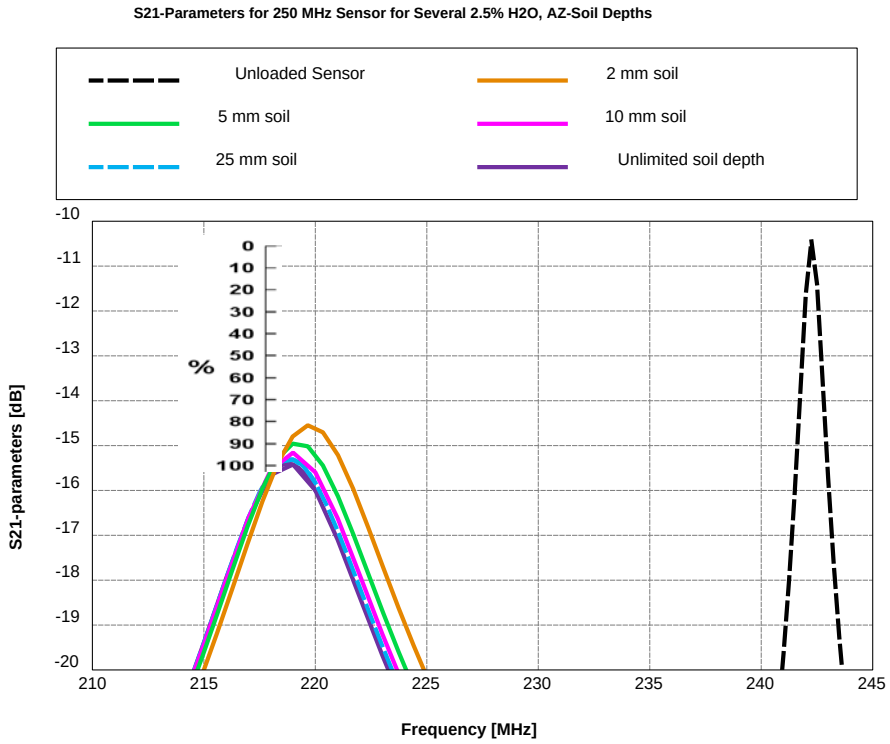

Fig. 25 Resonances for M250 with several 2.5% H_2O Arizona soil depths

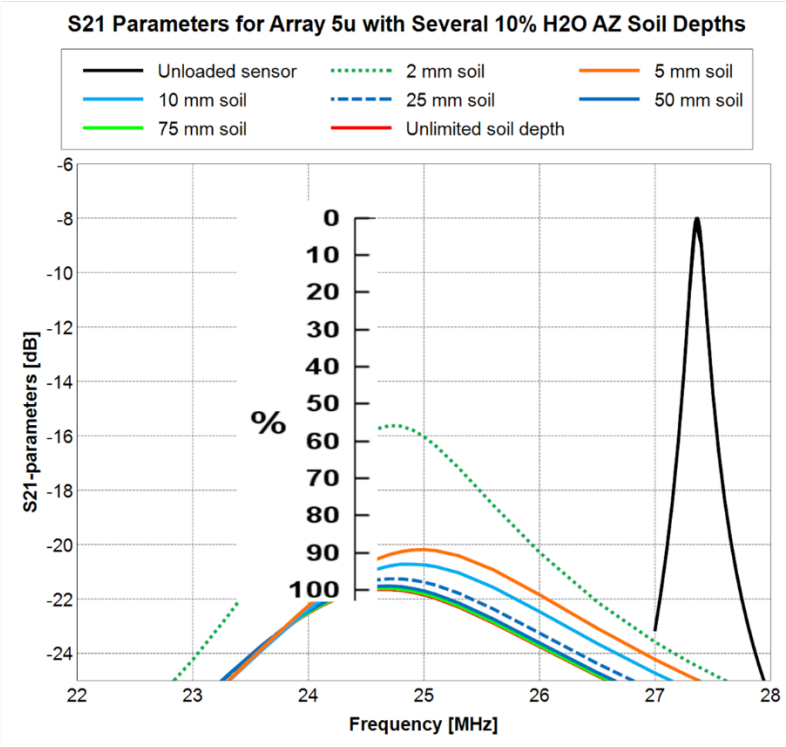

Fig. 26 Resonances for M5u with several 10% H_2O Arizona soil depths

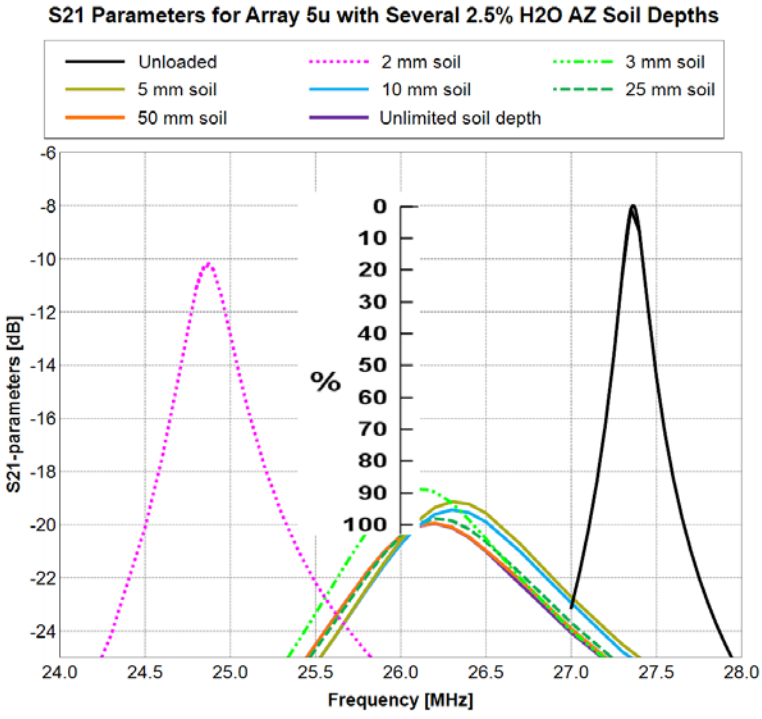

Fig. 27 Resonances for M5u with several 2.5% H_2O Arizona soil depths

Another way to characterize degree of agreement is through the changes in the measureable parameters from which the real and imaginary parts of the permittivity are determined. This second means of assessment is closer to our goal. The ratio of the resonance frequency of the loaded to unloaded sensor, f_l/f_u, is necessary for the determination of ε_r, while the additional parameter $\Delta(1/Q) \equiv 1/Q_l - 1/Q_u$, where the subscripts "$l$" and "$u$" represent the loaded and unloaded sensor cases, is needed to determine ε_i. Table 3 summarizes how well a given soil depth is able to represent the ideal or infinite depth case using these two techniques. Similarly, Table 4 shows the convergence of the sensor measurable parameters for permittivity evaluation with soil sample depth for Model 5u.

Table 3 Soil sample depth needed to agree with ideal measurement (at ∞ depth) for models A7 and r250

Model; AZ soil	Parameter	∞ Depth	25 mm	10 mm	5 mm	2 mm
A7; 10%H2O	%	**100**	99	94	89	74
	fl/fu	**0.901**	0.901	0.911	0.916	0.917
	Δ(1/Q)	**0.1130**	0.1115	0.1059	0.0993	0.0771
r250; 10%H2O	%	**100**	98	90	80	65
	fl/fu	**0.806**	0.807	0.809	0.812	0.817
	Δ(1/Q)	**0.0693**	0.0693	0.0690	0.0688	0.0668
A7; 2.5%H2O	%	**100**	99	93	90	77
	fl/fu	**0.959**	0.959	0.965	0.967	0.954
	Δ(1/Q)	**0.0368**	0.0371	0.0349	0.0326	0.0280
r250; 2.5%H2O	%	**100**	97	94	90	82
	fl/fu	**0.903**	0.903	0.904	0.905	0.907
	Δ(1/Q)	**0.0249**	0.0251	0.0253	0.0248	0.0243

Table 4 Soil sample depth needed to agree with ideal measurement (at ∞ depth) for model 5u

Model; AZ soil	Parameter	∞ Depth	75 mm	50 mm	25 mm	10 mm	5 mm	2 mm
5u; 10%H2O	%	**100**	100	99	97	93	89	55
	fl/fu	**0.901**	0.902	0.902	0.904	0.908	0.914	0.903
	Δ(1/Q)	**0.1197**	0.1207	0.1155	0.1177	0.1111	0.1308	0.0620
Model; AZ soil	Parameter	∞ Depth	50 mm	25 mm	10 mm	5 mm	3 mm	2 mm
5u; 2.5%H2O	%	**100**	100	98	96	93	89	18
	fl/fu	**0.957**	0.957	0.958	0.962	0.963	0.955	0.909
	Δ(1/Q)	**0.0387**	0.0394	0.0383	0.0373	0.0285	0.0327	0.0060

As is especially noticeable in the 2.5% H_2O Arizona soil cases for thin soil depths, near or below 5 mm of soil, the resonance becomes nonlinear. In a linear case one would expect the resonance curves to approach the unloaded case in height, width,

and position on the frequency spectrum as the soil thins. However, in cases with soil depths of 2 mm or less the resonance may swing radically from the linear response as we saw in several simulations shown in Fig. 27. In these thin soil depth cases, the S_{21} parameter response appears as though the resonance system has become overly sensitive to the soil depth condition or "chaotic". This nonlinear response is present, but less noticeable, in the small soil depths of Figs. 22, 24, and 26 for Models M7 and M5u. For the soils we have explored in this study, we conclude that use of a soil sample thickness of about 5 mm or less is unlikely to yield results from which one could correctly extrapolate the permittivity of the soil being tested.

The modeling in this study assumes a uniform or homogenous soil. In practice, soil is grainy to different degrees, and there may be pieces of organic material of different sizes and properties, further altering the effective permittivity. The nonlinear responses for the thin soil depth cases gives rise to the question as to whether certain kinds of graininess or inhomogeneities in soils to be tested with resonators could contribute to or cause errors in some such measurements via related nonlinear responses.

A soil depth of 25 mm or greater gives excellent agreement with the ideal case for these sensors in these two frequency ranges with these two soils. Convergence of the $\Delta(1/Q)$ parameter toward the unlimited depth is faster for the 200–220 MHz range than for the 35-MHz range as the soil depth is increased. No consistent difference between the two frequency ranges was noticed for the convergence of the F_l/F_u ratio.

Although sample depths of 25 mm or greater would be best to produce accurate measurements, Tables 3 and 4 data suggest that the first 5 mm of soil is responsible for about 90% or more of the changes in the $\mathbf{\Delta(}1/Q\mathbf{)}$ and F_l/F_u that determine the permittivity for our cases of homogeneous soils. Therefore one could conclude that the sensor is not looking deeply into the soil.

4. Summary and Conclusions

Meandered-line resonator designs for measurement of soil permittivity in the 20- to 90-MHz range were developed here with the aid of computational EM simulations. These designs are intended to give guidance on the construction for actual resonators as well as recommendations for soil sample or dielectric calibration thicknesses.

Initially we sought to reach our goal of modifying a computer model of a 250-MHz meander-line resonator into a 20- to 90-MHz range resonator model by increasing

the meander length of our resonator and using a high-dielectric substrate as in Rogers Corporation RO3010 to keep its areal footprint limited. We hit an impasse when that approach would not let us go below 77 MHz for the unloaded resonator. By increasing the thickness of the resonator substrate, we were able to push beyond the 77-MHz barrier. Each additional increase in thickness pushed F_0 still lower.

We revisited some of the models that had hit the barrier in our earlier modeling and by increasing substrate thickness, enabled them to reach into the 20-MHz decade. Most of these new models had better performance for moist soils than our first models that had reached into the 20-MHz decade. These new models typically had fewer loops, were smaller, and less lossy. From our sample of 11 resonators we found a lower bound on F_0 that can be described by $F_0 \geq 50.6\ h^{-1} - 2.14$. Moreover, since h and w are nearly linearly related to each other for our models and frequency range, we also found that $F_0 \geq 41.4\ w^{-1} - 0.98$**,** where h and w are in millimeters and F_0 is in megahertz.

Resonance strength with and without soil loading tended to be stronger by several decibels for models with fewer meander loops, possibly resulting from less energy loss from either the fewer loop ends or the smaller area of those sensors. Diminished higher-order resonances with soil loading appear to be consistent with greater energy loss into the soil with increasing frequency and also with greater losses for higher dielectric soils.[7]

Most of the models discussed in this report are able to measure soil permittivity down to the 20-MHz decade. Their success varied. One set of models produced several usable resonances closely spaced in frequency for dry soil but just one with possibly a second resonance for more moist soils, all at the low end of our band. These tended to be the large models with the most meanders. By contrast, another set of models produced a few strong resonances, for both dry and moist soils but at such wide separations that the entire 20- to 90-MHz band was covered. These models were smaller with much fewer meanders. Model M5u, with three strong resonances for all four soil moisture levels spanning our entire band, was the best of these models.

A part of the study to determine sufficient soil sample depths indicated on the one hand that about 90% of the effect from which the permittivity could be determined occurred within the first 5 mm of soil from the face of the sensor. On the other hand, it concluded that homogenous soil or dielectric samples for such resonators needed to be at least 25 mm deep against the face of the resonator to give an excellent (98% or 99%) agreement with the ideal of unlimited soil depth. Some soil samples with depths from about 5 mm or less showed interesting nonlinear responses that would result in very erroneous permittivity determinations. This

nonlinear error rapidly increased with decreasing soil sample depths starting at near 2 mm.

These simulation studies led to some puzzling aspects concerning the resonances found in the model, which we leave unanswered here. For example, what is the cause or explanation for the lower bound dependence upon substrate thickness or line width? A broad and deep "canyon" in the S_{21} versus frequency curves preceded the "first" resonance in each of our cases. These canyons essentially rendered as vestigial anything that otherwise might be a resonance within or before that canyon. How is that canyon related to the substrate thickness or line width? Why are the resonances so close to each other as the number of loops gets very large? The number of potential resonances seems to become much more than the number of possible multiple lengths of the resonator, even considering an effective dielectric constant for the resonator. Considering the 10-MHz or less separation between resonances, one might expect that F_0 would be equal to this separation. The M5 models with their shorter loop lengths, including our favored M5u, seem to have escaped the conundrum about the large discrepancy between resonance separation sizes and F_0.

6. References

1. Mazzaro G, Sherbondy K, Smith G, Ressler M, Harris R. Portable ring-resonator permittivity measurement system: design and operation. Adelphi (MD): Army Research Laboratory (US); 2012 Apr. Report No.: ARL-TR-5993.

2. Altair FEKO. Altair HyperWorks: Altair FEKO overview. Troy (MI): Altair Engineering, Inc [accessed 2018 Apr 20]. https://altairhyperworks.com /product/FEKO.

3. Rogers Corporation. RO4000 series high frequency circuit materials data sheet. Chandler (AZ): Advanced Connectivity Solutions [accessed 2018 Apr 20]. http://www.rogerscorp.com/documents/726/acs/RO4000-LaminatesData-Sheet.pdf.

4. Rogers Corporation. RO3000 series circuit materials data sheet. Chandler (AZ): Advanced Connectivity Solutions [accessed 2018 Apr 20]. http://www.rogerscorp.com/documents/722/acs/RO3000-Laminate-Data-Sheet-RO3003-RO3006-RO3010-RO3035.pdf

5. Carin L, Geng N, McClure M, Sichina J, Nguyen L. Ultra-wide-band synthetic-aperture radar for mine-field detection. IEEE Antennas and Propagation Magazine. 1999 Feb;41(1).

6. Smith, GD. VHF/UHF UWB SAR related permittivity measurements using the Damaskos 3000T measurement system. Adelphi (MD): Army Research Laboratory (US); 2003 Aug. Report No.: ARL-TR-3044.

7. Steinberg BK, Levitskaya TM. Electrical parameters of soils in the frequency range from 1 kHz to 1 GHz, using lumped-circuit methods. Radio Science. 2001 July/Aug;36(4).

List of Symbols, Abbreviations, and Acronyms

EM	electromagnetic
H_2O	water
I/O	input/output
MoM	Method of Moments
Q	quality factor
RF	radio frequency

1 (PDF) DEFENSE TECHNICAL INFORMATION CTR DTIC OCA

2 (PDF) DIR ARL
IMAL HRA
RECORDS MGMT
RDRL DCL
TECH LIB

1 (PDF) GOVT PRINTG OFC
A MALHOTRA

1 (PDF) CITADEL
G MAZZARO

8 (PDF) ARL
RDRL SER U
C KENYON
K SHERBONDY
K GALLAGHER
B PHELAN
G KIROSE
G SMITH
A SULLIVAN
T DOGARU